Hindawi
International Journal of Antennas and Propagation
Volume 2022, Article ID 4886844, 12 pages
https://doi.org/10.1155/2022/4886844

Research Article

Design of UWB Wearable Conformal Antenna Based on Jean Material

Peng Chen,[1] **Dan Wang**,[1] **Lu Liu**,[1] **Lihua Wang**,[1] **and Yumeng Lin**[2]

[1]*School of Ocean Information Engineering, Jimei University, Xiamen 361005, China*
[2]*College of Navigation, Jimei University, Xiamen 361005, China*

Correspondence should be addressed to Peng Chen; chenpeng@jmu.edu.cn

Received 27 May 2022; Revised 10 July 2022; Accepted 18 July 2022; Published 23 August 2022

Academic Editor: Sandeep Kumar Palaniswamy

In this paper, a wearable ultra-wideband (UWB) microstrip antenna is designed to meet the demand for Wireless Body Area Network (WBAN). This is a wearable textile antenna, which was formed on a jeans fabric substrate to reduce surface-wave losses. The single-fed circular strip monopole antenna provides good impedance matching over the entire UWB frequency range of 2.9~10.6 GHz. The dielectric constant $\varepsilon_r = 2.2$, and the loss tangent $\tan\delta = 0.04$ of the jean substrates are measured by using the coaxial ring method. The proposed antenna consists of an improved circular radiation patch with the defective ground structure to expand the frequency band of the antenna and improve the radiation characteristics of the antenna with small dimensions of $20 \times 30 \times 1.4\,\text{mm}^3$. In addition, structural deformation of the proposed antenna is performed to analyze the flexibility of the proposed antenna. The simulated SAR values follow the FCC limit, making it most suitable for wearable applications.

1. Introduction

WBANs are networks distributed around the human body. WBAN is mainly used to detect and transmit the user's physiological data and cooperates with other networks to integrate the human body into the overall network [1]. Nowadays, wearable electronics are becoming popular and usability, functionality, durability, safety, and comfort have become essential elements of wearable systems [2]. The potential applications of wearable antennas for tracking, navigation, public safety, and health monitoring are also increasing [3]. In military applications, wearable antennas can provide personal positioning and mobile communication through helmets [4, 5]. In healthcare, wearable antennas can monitor physiological information, such as blood pressure, blood glucose concentration, temperature, weight, and heartbeat [6–8]. These applications face limitations due to electromagnetic coupling between the human body and the antenna, changing physical deformations, highly variable operating environments, and manufacturing processes [9–11].

Wearable systems require antennas as transmitters and receivers. Bending and stretching of flexible and wearable antennas during use not only affects resonance frequency but also the radiation characteristics of the wearable antenna, especially when it requires circular polarization. Flexibility, lightweight, comfort, and robustness are essential features for designing wearable antennas [12]. Textile antennas are therefore a strong candidate for wearable applications. Textile-based antennas with easy integration with clothing and without interfering with the user; various textile materials such as flannel, felt, denim, polyester, and cotton have been used as substrates. The relative dielectric constant of the fabric material is between 1.05 and 1.9, and the loss tan σ is between 0.0001 and 0.025, which depends on the working frequency, moisture content, fabric structural properties, and bulk density of the fabric material [13]. A felt-based wearable antenna for 2.4/5.2 GHz dual-band operation in WLAN applications with a maximum gain of 1.8 dBi/3.2 dBi has been proposed in [14]. Polyester and denim textiles have been used in wearable antennas that provide a frequency range of 2.25~2.74 GHz and 4.3~6.8 GHz for WLAN and WiMAX band applications [15]. In comparison, the inherent flexibility and lightweight properties of denim materials can provide more convenience

for users in real-time environments [16, 17]. In [18], a circular slotted textile antenna with a partially grounded structure with an impedance bandwidth of approximately 46% and 41%, respectively, has been proposed. Its results show that denim fabrics are good candidates for textile wearable applications. Denim fabric is also one of the best choices for designing UWB circular patch antennas [19, 20]. It has been observed that the antennas are designed using complex structures of radiators to cover the target frequency range [14, 21]. Wearable antennas do not have structural deformations, and human experiments analyze the changes in antenna performance [18–24]. The antenna [17, 20] results in a large antenna dimension and increases the design complexity of the receiver front-end systems. The proposed antenna overcomes the above-mentioned issues and provides novel features such as a compact, simple structure, and covers the entire UWB frequency range. The antenna sustains its performance in terms of impedance bandwidth, radiation pattern, and current distribution even when tested on body tissues suitable for on-head communication.

In this paper, a wearable antenna with an improved circular patch for WBAN is proposed, which uses denim fabric as the substrate and consists of a circular radiating patch with a square slot in the middle, a rectangular microstrip line, and a defective ground structure to achieve the coverage of the whole UWB frequency range from 3.1 GHz to 10.6 GHz. A stable omnidirectional radiation pattern is obtained with the required gain and efficiency over the entire UWB frequency range. The antenna is small in size, bendable, easy to integrate, easy to process, and suitable to be integrated to wear on a hat.

2. Antenna Structure and Design

2.1. Fabric Characterization. The transmission-reflection method has the advantages of easy operation and fast measurement speed. The method can be divided into the coaxial circular method and the rectangular waveguide method according to the different measurement fixtures. The coaxial circular method has a wide range of measurements and is easy to prepare specimens; the rectangular waveguide method requires separate measurements of each waveband and is more complicated to prepare specimens. Therefore, in this paper, the coaxial circular method of transmission reflection is used to measure the dielectric constant of denim fabrics.

The coaxial ring method is used to measure the electromagnetic parameters of the denim fabric, and the test sample needs to be calibrated with mechanical or automatic calibration parts before testing. After the calibration is completed, a circular sample with the same inner and outer diameter is prepared with a grinding tool and placed in the fixture. The instrument emits a wave signal of a specific frequency through one port, which is reflected in the fixture containing the sample through the transmission to respond. Then the other end of the cable is transmitted back to the instrument for analysis and calculation, and finally, the computer can directly display the electromagnetic parameters of the material. [25, 26].

The dielectric constant of denim fabric is $\varepsilon_r = \varepsilon' - j\varepsilon''$. The magnetic permeability of denim fabric is $u_r = u' - ju''$. ε', ε'' are the real and imaginary parts of the dielectric constant of the material, respectively. u', u'' are the real and imaginary parts of the magnetic permeability of the material. Dielectric loss tangent is $\tan\delta = (\varepsilon''/\varepsilon')$.

This paper uses the Keysight N5222 B Vector Network Analyzer (VNA) mainly to measure ε', μ', and μ''. A schematic diagram of electromagnetic property measuring equipment is shown in Figure 1(a). A de-embedding technique that compensates both phase and magnitude was used to get the S-parameter of the device under test (DUT), which is shown in Figure 1(b). The relative permittivity and permeability of the material as a function of frequency are given in Figure 2. Thus, the substrate used in the proposed antenna has a relative permittivity of 2.2, a permeability of 1.0, and a loss tangent of 0.04.

2.2. Evolution of Antenna. Different from the previous studies of UWB antennas [27–30], the ultra-wideband microstrip antenna designed in this paper is made of jean cloth as the medium substrate, a circular radiation patch with a square slot in the middle, a rectangular microstrip line, and a defective ground structure. The antenna is a circular patch antenna with an open rectangular slot in the middle, which can generate ultra-wideband operating frequency bands through its resonance characteristics. Compared with the triangular or elliptical gap ultra-wideband, the antenna has more adjustable dimensional parameters due to its defective structure, making it easier to achieve impedance matching. This type of defect plays an important role in the bandwidth and wideband characteristics of the antenna.

The structure of the circular ultra-wideband antenna designed in this article is shown in Figure 3. The dielectric substrate is $20 \times 30 \times 1.4\,\text{mm}^3$, and studies on all impedance matching have resulted in a 50 Ω microstrip feeder for antenna feed achieved by the HFSS 19.0. The key parameters of the antenna are optimized with the optimization goal of performance and impedance matching, and the specific antenna size parameters are shown in Table 1.

As shown in Figure 4, the design process of the ultra-wideband antenna structure is described in this paper. Figure 5 and Figure 6 show the s11 and surface current distribution of the antenna at different stages. Figure 4(a) depicts the original structure of the antenna design, using a 50 Ω rectangular microstrip line, a circular radiation patch, and a rectangular ground plate. The antenna model is a simple and small-size antenna. The original model's working band is 3.5 GHz to 10 GHz and 10.3 GHz to 14.5 GHz (stage 1).

Rectangular slots are cut in the antenna base plate and asymmetric rectangular slots are cut in the center of the circular radiating patch at stage 2. After adding slots, the current paths have been changed by the inserted structures at 8 and 10 GHz separately. It can be observed that the current flowing through the slot becomes larger, causing a slight shift in the resonant frequency point of stage 2

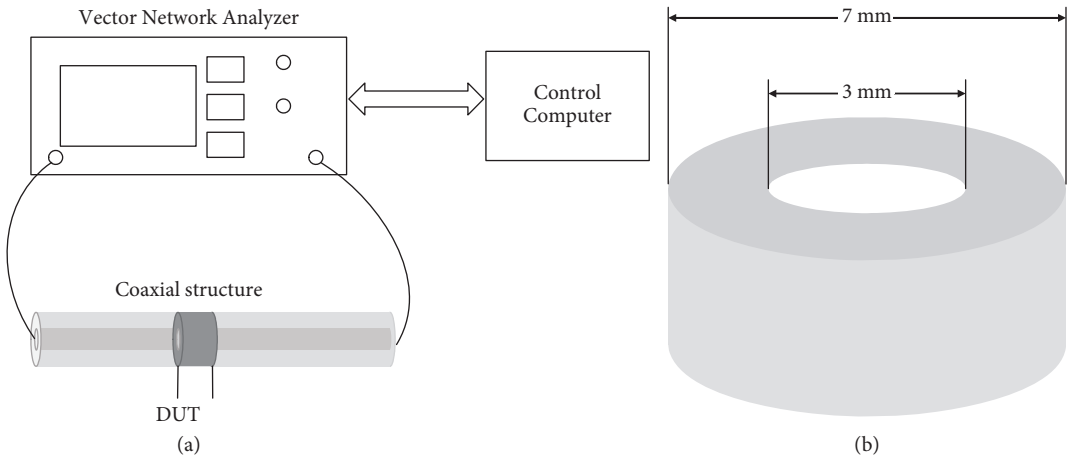

Figure 1: Schematic diagram of electromagnetic property measuring equipment and sample: (a) equipment for coaxial ring method test; (b) DUT.

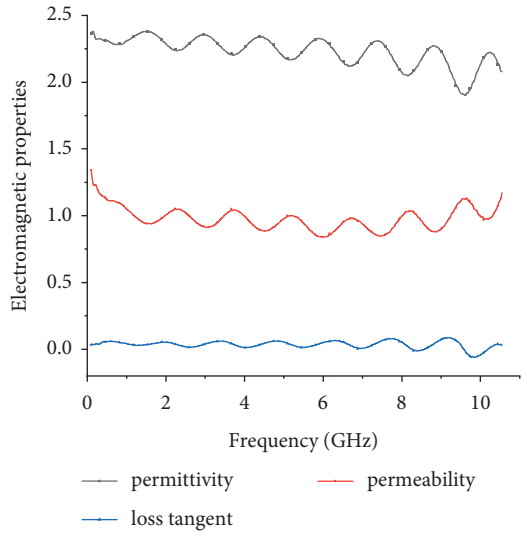

Figure 2: Measured permittivity and permeability.

compared to stage 1. The operating bandwidth of the antenna is set to be 3.4 GHz to 9.6 GHz and 11.1 GHz to 14.6 GHz.

Based on structure 2, rectangular slots are added in the center of the circular radiation patch and grounding plate. The operating bandwidth of the antenna is further improved so that the return loss is less than −10 dB in the bandwidth from 3.42 GHz to 15 GHz (stage 3). However, some low-frequency parts are still not covered in the UWB (3.1~10.6 GHz).

Based on structure 3, the upper edge is detriangulated to obtain the final model of the antenna (stage 4). After the slotting, the working bandwidth of the antenna is extended to a certain degree in the low-frequency part, and the working bandwidth of the antenna is from 2.9 GHz to 15 GHz, which meets the communication requirements of the UWB. The simulated reflection coefficient characteristics of the evolution of the proposed antenna are shown in Figure 5.

The current distribution results bring to light the idea of understanding how the current flows in the conductive region of the simulated UWB wearable antenna. Figure 7 shows these results for the proposed antenna design using denim fabric as the substrate along with copper as the conductor material. The antenna bends on a cylindrical model with a radius of 50 mm. Simulate and measure thebending in the X and Y directions and observe the results. For discussion samples at 4 GHz, 6 GHz, and 8 GHz for three different frequencies have been provided. As can be seen from Figure 8, the intensity of the current is high in the frequency range from 4 GHz to 6 GHz. The high-intensity currents at 4 GHz and 6 GHz are found to be radiated along the conductive part of the antenna, especially along the transmission line as well as in the middle of the circular patch. On the other hand, at 8 GHz, high current intensity was found at both ends of the transmission line and at the bottom of the circular patch.

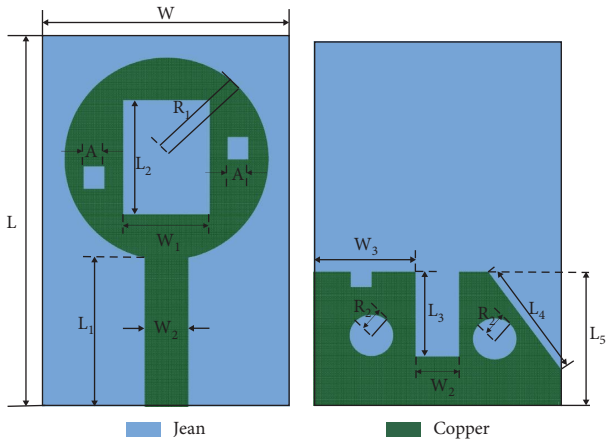

Figure 3: Geometry of the proposed antenna. (a) Front view. (b) Rear view.

2.3. Fabrication. The antenna is based on denim fabric with copper as the conductive material. Due to the limitations of

Table 1: Antenna basic size parameters.

Parameters	Sizes (mm)	Parameters	Sizes (mm)	Parameters	Sizes (mm)
W	20	L	30	L_4	10
W_1	6	L_1	12	L_5	10
W_2	3.5	L_2	8	R_1	8.1
A	1.4	L_3	5.5	R_2	1.4

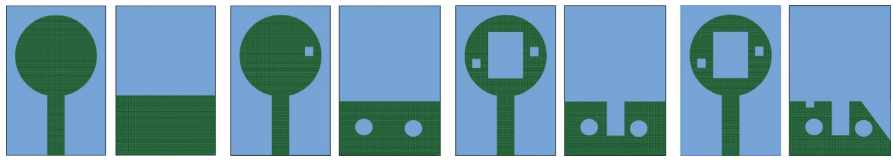

Figure 4: The design process of the UWB antenna. (a) Round monopole antenna. (b) Slotted circular antenna. (c) Microstrip antenna with rectangular slot. (d) Improved circular microstrip antenna with asymmetric defect ground.

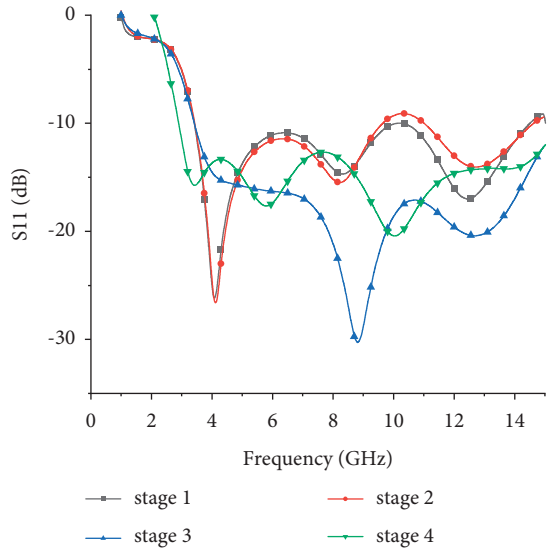

Figure 5: Simulated reflection coefficient of the evolution of the antenna.

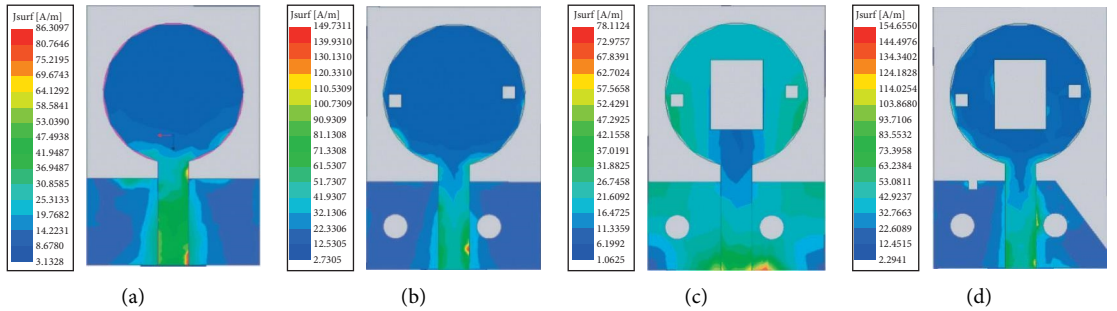

Figure 6: Simulation results of the current distribution of the UWB antenna with a phase of 0: (a) stage 1, (b) stage 2, (c) stage 3, and (d) stage 4.

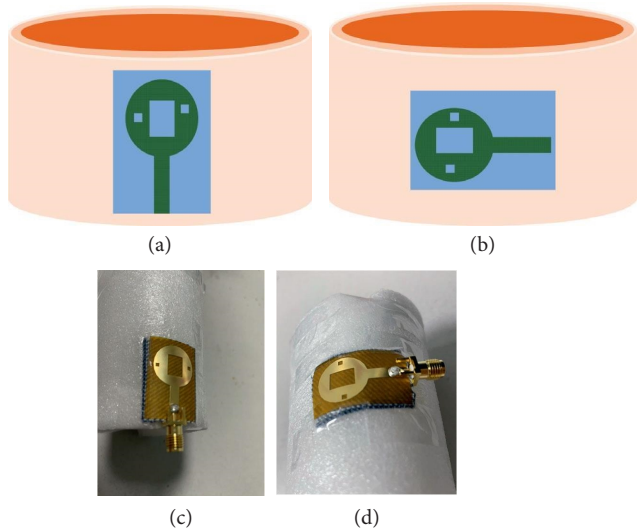

Figure 7: Structural deformation. (a) Simulated X-bend. (b) Simulated Y-bend. (c) Measured X-bend. (d) Measured Y-bend.

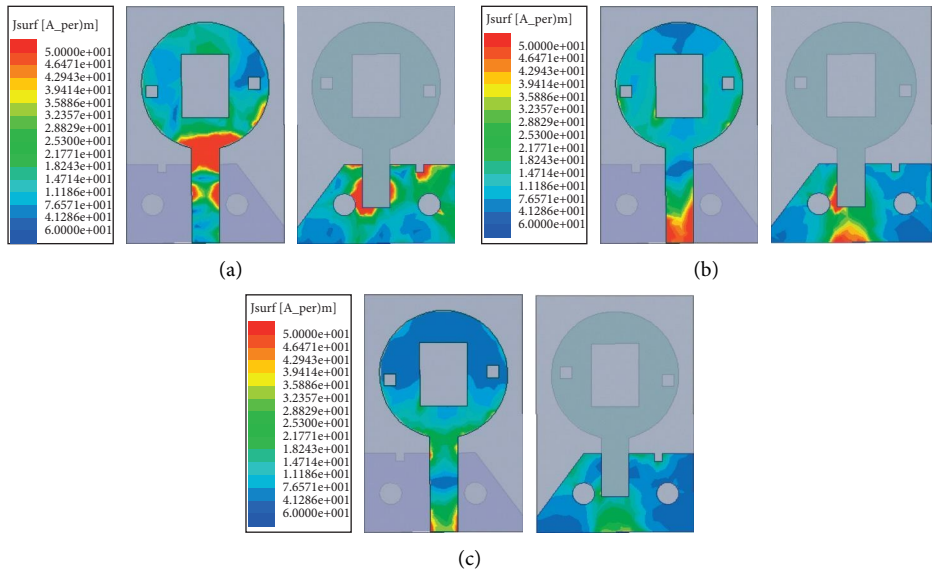

Figure 8: Simulation results of the current distribution of UWB antenna in free space for three different frequency samples: (a) 4 GHz, (b) 6 GHz, and (c) 8 GHz.

the process, copper cannot be directly attached to the fabric substrate. The adhesion of the conductive material to the fabric substrate is very important. Therefore, copper was chosen to cover the FPC flex board. In other words, the radiating patch and ground are covered on the FPC flex board, and the substrate is sandwiched between the flex boards so that the conductive material is evenly placed on the denim and fixed. It forms an antenna structure with radiant elements and FPC flexible board as the top layer, jean fabric as the substrate material, and FPC flexible board and grounding metal as the bottom layer. The specific dimensions are shown in Table 2. In antenna fabrication, direct metal soldering is used to connect the top radiating patch and ground plane to the coaxial connector. Antennas are manufactured to meet the requirements of the wearer's demands for compact size, flexible materials, easy to clean, and very attractive wearable devices.

3. Results and Discussion

The performance of the antenna is analyzed by using parameters such as reflection coefficient, radiation pattern, gain, and efficiency. The fabricated prototype of the proposed antenna is shown in Figure 9. The simulation is performed using the HFSS 19.0 and measurements are

Table 2: Dimensions of the designed wearable UWB antenna.

Location	Substrate thickness (mm)	Substrate dimensions (mm)	FPC thickness (mm)	FPC dimensions (mm)
Sizes	1	20 × 30	0.2	20 × 30

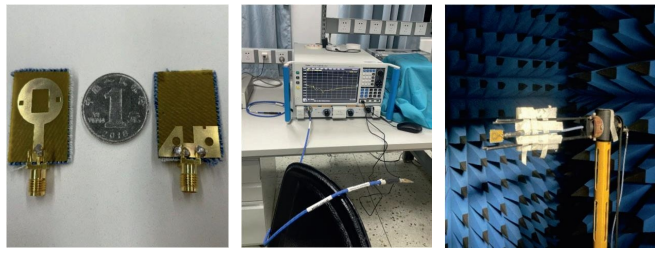

(a) (b) (c)

Figure 9: (a) Fabricated textile antenna front and back view. (b) Vector network analyzer. (c) Radiation pattern measured in free space.

carried out using Keysight's 3672D Vector Network Analyzer.

3.1. Measurement and Simulation Results. The effect on the antenna performance can be evaluated with the human brain model of the human body structure that comes with HFSS. However, the human brain model has a very dense mesh with distinct contour features and a long simulation time. To simplify the study environment, a spherical container and brain tissue fluid are used to simulate a simple human head model. The relative permittivity of the brain tissue fluid is 41.5 with a loss tangent of 0.90, and the relative permittivity of the shell is 4.6 with a loss angle tangent of 0.01.

As shown in Figure 10, the simple human head model has a hollow spherical shell with a radius of 111.5 mm and a thickness of 5 mm. The brain tissue fluid is a spherical model with a radius of 106.5 mm. The results were observed by placing the antenna on the head of a human volunteer with a height and weight of 155 cm(45 kg) for measurement. Considering that the antenna is wearable, the distance between the antenna and the manikin is kept at 10 mm.

The simulation of the proposed antenna provides a frequency range from 2.9 GHz to 15 GHz. The anthropometric results provide a frequency range of 2.8 GHz to 10.8 GHz. Figure 11 shows a comparison of the characteristics of the simulated and measured reflection coefficients in free space and in the human body. However, free space and physical outcomes are interrelated, and even though the actual bandwidth of the antenna becomes smaller, it still covers the entire ultra-wideband frequency range. The slight change between simulated and measured results is due to the flexibility of the textile material, fabrication tolerance, humidity, and temperature effect on cotton. However, simulated and measured results show a good correlation.

The radiation patterns are measured in the anechoic chamber. Figure 12 depicts a comparison of the simulated and measured normalized directional maps of the proposed antenna in the YOZ-plane and XOZ-plane of the free space at different frequencies, such as 4 GHz, 6.5 GHz, and 8 GHz.

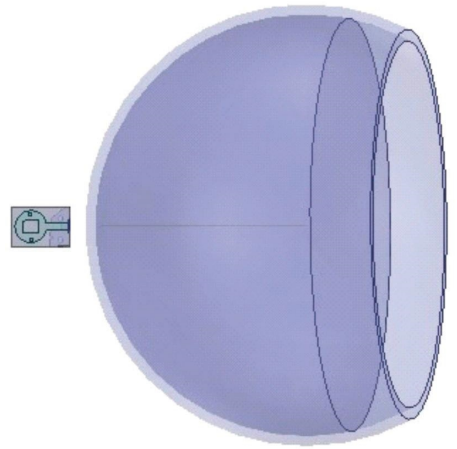

Figure 10: The simulation model of the human brain.

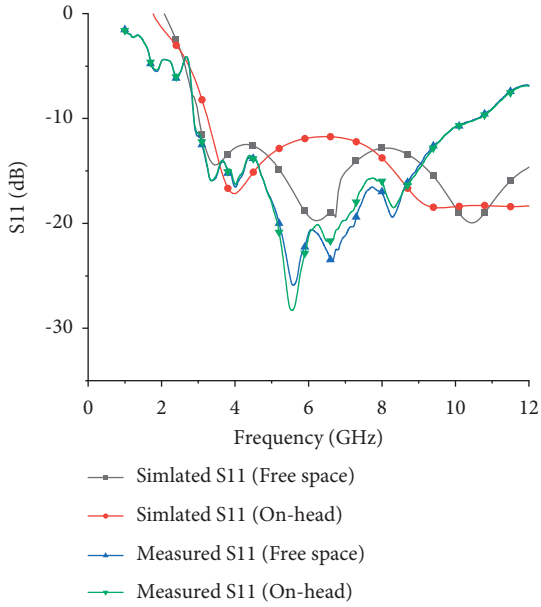

Figure 11: Simulates and measures the reflective coefficient of the proposed antenna in free space and on the human body.

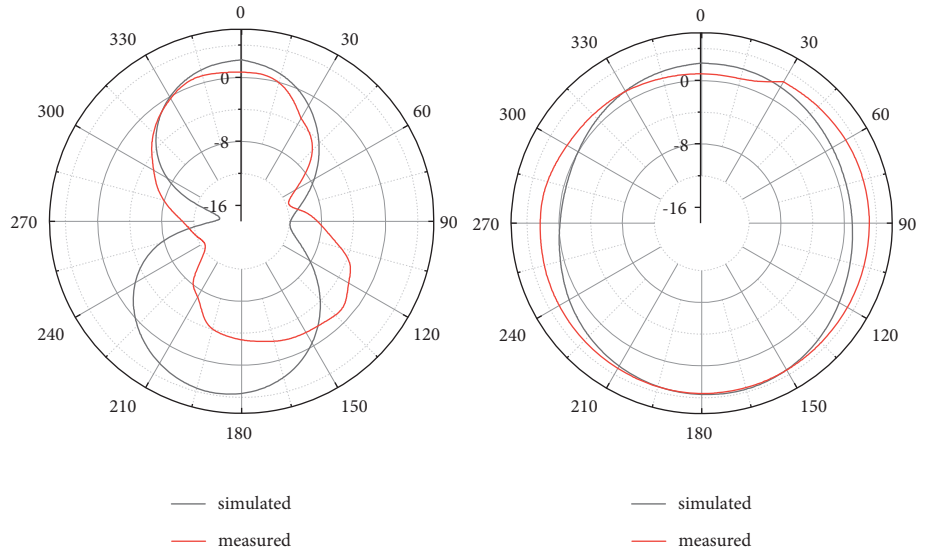

(a)

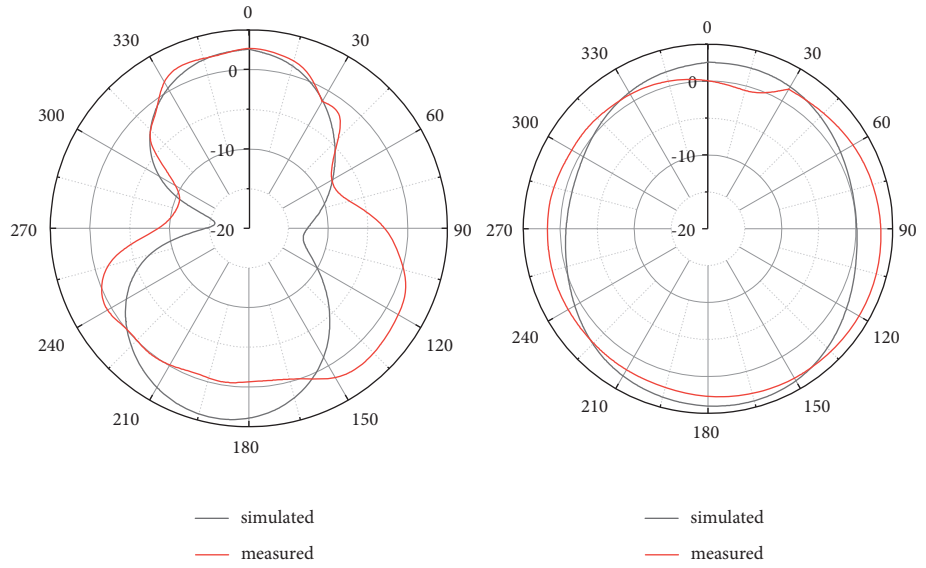

(b)

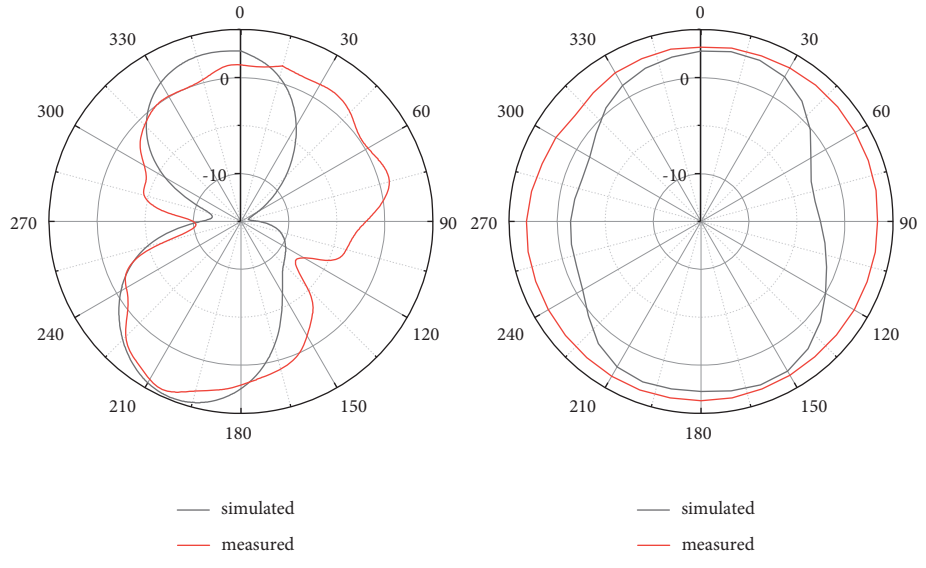

(c)

FIGURE 12: Free space comparison of simulated and measurement radiation pattern in the YOZ-plane and XOZ-plane. (a) 4 GHz. (b) 6.5 GHz. (c) 8 GHz.

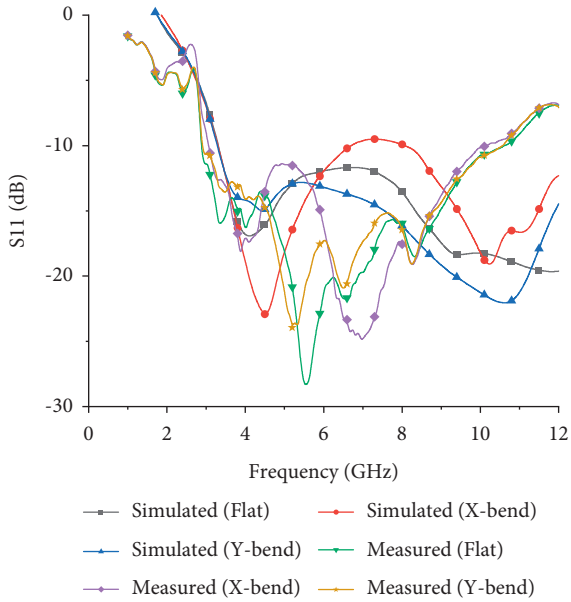

Figure 13: Comparison of the characteristics of the simulation and measurement of reflection coefficients caused by structural deformation on the human head.

A stable radiation pattern is observed over the entire frequency range. It can be observed from the figure that the proposed antenna has omnidirectional radiation in the XOZ-plane.

3.2. Structural Deformation. It is difficult to keep the antenna flat at all times in wearable systems, especially when the antenna is made of textile materials. Since the designed antenna is integrated into a cowboy hat, it is necessary to study the performance characteristics of the antenna under bending conditions. When the antenna is placed on the human body, the antenna performance will be strongly affected due to the electromagnetic coupling and specific absorption of the human body. The high dielectric constant and conductivity of human tissue affect the performance and propagation loss of the antenna. Therefore, the analysis of the structural deformation is necessary to better understand the flexible characteristics of the antenna.

Figure 13 provides a comparison of the simulated and measured reflection coefficient characteristics due to structural deformation with the conditions of bending in the *y*-direction on the human body model. From the figure, it can be concluded that the proposed antenna has a slight shift in the resonance point in the *Y*-direction bending towards the high frequency. It still covers the entire UWB (3.1 to 10.6 GHz), compared to the results obtained on the planar model. In the simulations and measurements under flat conditions, the measured antenna covers the frequency range from 2.9 GHz to 10.6 GHz with better impedance matching compared to the simulated results. Even though the proposed antenna is slightly shifted in the *Y*-direction bending the human head experiment, it provides an acceptable band coverage from 3.1 GHz to 10.2 GHz.

Figure 14 provides the normalized radiation patterns of the YOZ-plane and XOZ-plane due to structural deformation simulated on the human body. The radiation patterns obtained under the X-directional bending condition show slight deviations, but they still provide the required XOZ-plane omnidirectional radiation pattern for human body communication at different frequencies such as 4 GHz, 6 GHz, and 8 GHz. Therefore, the gain and efficiency obtained for the proposed antenna under the structural deformation with bending in the *X*-direction are small compared to the results for the free space variation as shown in Table 3. The proposed antenna still maintains its characteristics in terms of impedance bandwidth, radiation pattern, gain, and efficiency under structural deformation in the WBAN application situation.

3.3. Analysis of Specific Absorption Rate. Electromagnetic waves emitted by antennas cause radiation to penetrate the human body. SAR is the electromagnetic power absorbed or consumed by a unit mass of human tissue in W/kg. Different national organizations have different SAR limit standards. These standards recommend safe levels of radio radiation for the public as well as for workers. The SAR limits set by the FCC are 1.6 W/kg for 1 Gram of tissue and 2 W/kg for 10 grams of tissue. Wearable antennas must meet the safety limits. The distance between the antenna and the human head model is maintained at 10 mm. Figure 15 illustrates the 3D SAR distribution of the proposed antenna at 4 GHz, 6 GHz, and 8 GHz resonance frequencies in the head position with the maximum SAR values of 1.86 W/kg, 1.74 W/kg, and 1.52 W/kg for 10 g of tissue, respectively. Thus, the proposed antenna provides a limited SAR value that makes it most suitable for real-time applications.

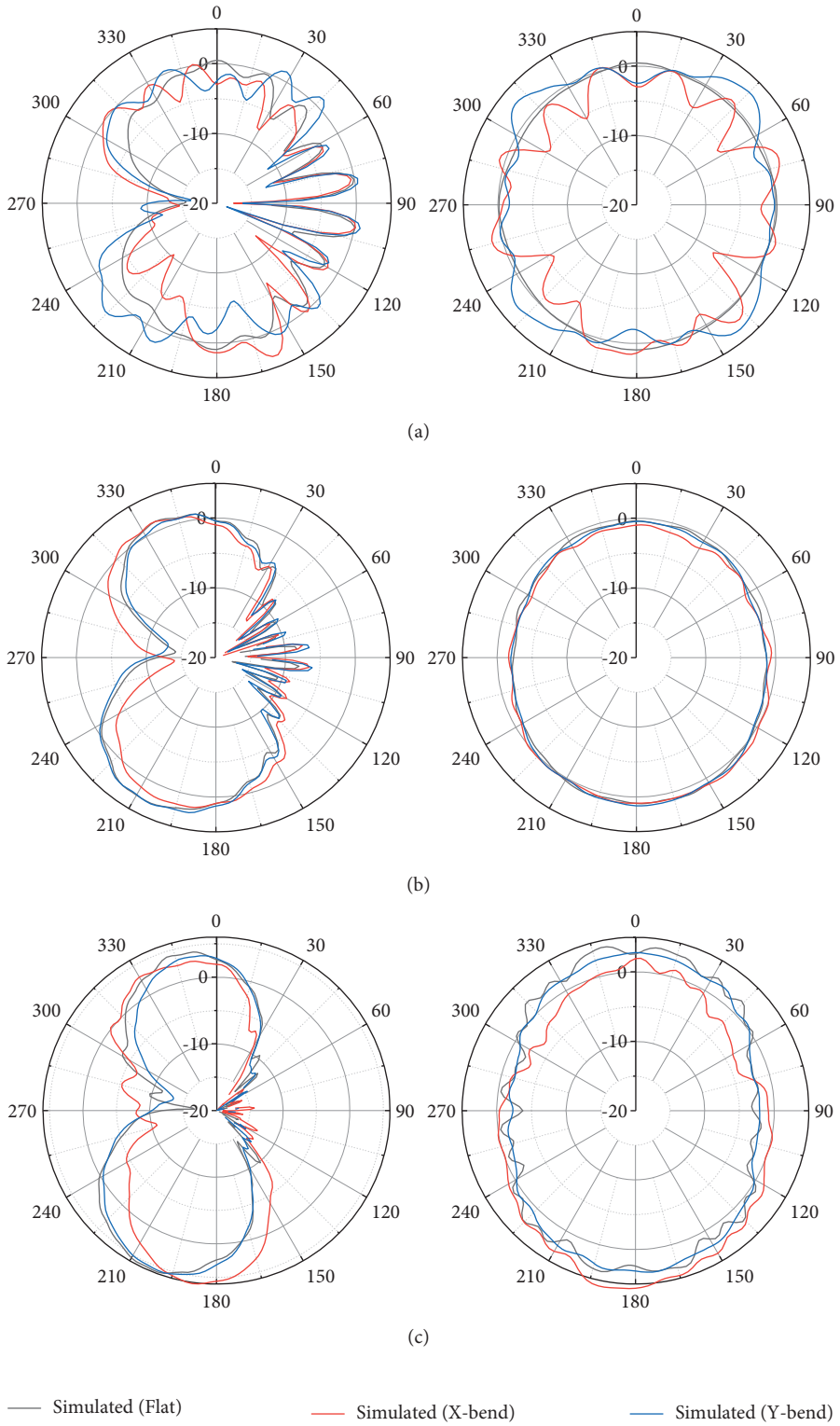

FIGURE 14: Comparison of simulated radiation patterns on the human head due to deformation of different structures in the YOZ-plane and XOZ-plane. (a) 4 GHz. (b) 6 GHz. (c) 8 GHz.

After investigating and evaluating the proposed antenna's performance under various conditions, it can be concluded that the proposed antenna is a reliable candidate as a wearable device for the WBAN.

Table 4 illustrates the close comparison of the proposed work with some recent similar works. It shows that the proposed antenna achieved a wider BW and higher radiation efficiency. The proposed antenna obtained these outcomes

Table 3: Simulated gain and radiation efficiency of the antenna after structural deformation.

Frequency (GHz)	Flat position		*X*-orientation		*Y*-orientation	
	Gain (dB)	Efficiency (%)	Gain (dB)	Efficiency (%)	Gain (dB)	Efficiency (%)
3	1.51	92.5	1.04	91.7	1.08	92.6
4	1.84	91.9	1.56	91.85	1.61	92.2
5	1.92	88.1	2.17	87.7	1.95	88.4
6	2.16	88.2	2.3	87.5	2.33	88.3
7	2.64	90.5	2.7	86.2	2.78	88.3
8	2.68	88.0	3.02	82.8	3.03	85.4
9	2.62	84.9	3.12	82.6	3.02	85.6
10	3.03	83.7	2.87	81.9	2.70	85.3
11	2.82	79.3	2.44	78.3	2.80	85.2

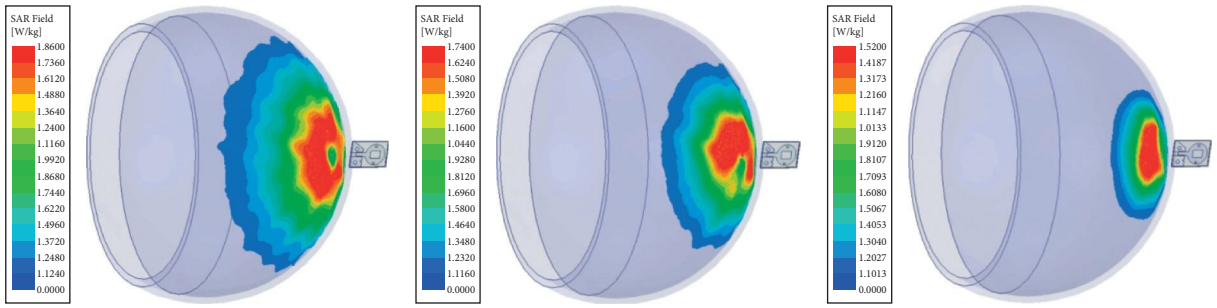

(a) (b) (c)

Figure 15: SAR analysis. (a) 4 GHz. (b) 6 GHz. (c) 8 GHz.

Table 4: Comparison with existing literature.

Ref no.	Sizes (mm)	Radiator	BW (GHz)	Substrate	Max radiation efficiency (%)	Max gain (dBi)
[22]	25 × 30	Modified octagonal strip monopole antenna	3.1–10.6	Jeans	82	4.4
[21]	88 × 97	Fully textile microstrip topology	3–10	Felt	62	7.75
[18]	40 × 40	Octagonal slot-loaded circular-shaped textile antenna	3.01–5.30 8.12–12.35	Jeans	94	5.7
[31]	67 × 80	Two modified arc-shaped patches antenna	3.7–10.3	PDMS	45	5
[20]	60 × 60	Fully textile materials antenna	3–20	Flannel	97	7.4
[32]	70 × 70	Aperture-stacked patch antenna	3–6	Rogers	48	-
[33]	50 × 60	Full ground UWB antenna	7–28	Jeans	96	10.5
[34]	56 × 70	Rectangular radiating patch antenna	3.6–11.3	Jeans	-	3.57
Proposed	20 × 30	Modified circular radiating patch antenna	2.9–10.6	Jeans	92.6	3.12

with smaller dimensions (it should be mentioned that the width of an antenna plays a direct impact on its efficiency and BW: when an antenna has larger dimensions, both gain and efficiency increase [33]).

4. Conclusions

An ultra-wideband wearable conformal antenna based on jean fabric is designed. The antenna satisfies the WBAN requirements and uses denim fabric as the substrate, which can be integrated into a hat. The proposed antenna provides good impedance matching throughout the UWB frequency range through a circular radiating patch with a rectangular slot in the middle, a rectangular microstrip line, and a defective ground structure. While examining the performance of the antenna under bending and on the head, a slight shift in resonant frequency is observed. The antenna has the features of small size, easy integration, bendability, and low impact on antenna performance when placed in front of a human head, which makes it a wearable antenna with use-value. For the proposed structure, the SAR obtained is 1.86 W/Kg below the recommended value, and the SAR value should be reduced further.

Data Availability

The data used to support the findings of this study are available from the corresponding author upon request.

Conflicts of Interest

The authors declare that they have no conflicts of interest.

Acknowledgments

This work was supported by the Natural Science Key Foundation of Fujian Province, Grant No. 2020J02042, Research on Integration Design and Industrialization of RF Components for 5G Wireless Communication Terminal, Grant No. S22042, and the Natural Science Foundation of Fujian Province of China. Grant no. 2021J05179.

References

[1] H. L. Yang, W. Yao, Y. Yi, X. Huang, S. Wu, and B. Xiao, "A dual-band low-profile metasurface-enabled wearable antenna for WLAN devices," *Progress in Electromagnetics Research C*, vol. 61, pp. 115–125, 2016.

[2] G. Cho, S. Lee, and J. Cho, "Review and reappraisal of smart clothing," *International Journal of Human-computer Interaction*, vol. 25, no. 6, pp. 582–617, 2009.

[3] M. E. B. Jalil, M. K. Abd Rahim, N. A. Samsuri et al., "Fractal koch multiband textile antenna performance with bending, wet conditions and on the human body," *Progress in Electromagnetics Research*, vol. 140, no. 140, pp. 633–652, 2013.

[4] H. Lee, H. Yang, S. Myeong, and K. Lee, "Dual-band MNG patch antenna for smart helmet," *Electronics Letters*, vol. 54, no. 19, pp. 1101-1102, 2018.

[5] A. S. M. Alqadami, A. Trakic, A. E. Stancombe, B. Mohammed, K. Bialkowski, and A. Abbosh, "Flexible electromagnetic cap for head imaging," *IEEE Transactions on Biomedical Circuits and Systems*, vol. 14, no. 5, pp. 1097–1107, 2020.

[6] A. Abdi, F. Ghorbani, H. Aliakbarian, T. K. Geok, S. K. A. Rahim, and P. J. Soh, "Electrically Small Spiral PIFA for Deep Implantable Devices," *IEEE Access*, vol. 8, 2020.

[7] A. S. M. Alqadami, K. S. Bialkowski, A. T. Mobashsher, and A. M. Abbosh, "Wearable electromagnetic head imaging system using flexible wideband Antenna array based on polymer technology for brain stroke diagnosis," *IEEE transactions on biomedical circuits and systems*, vol. 13, no. 1, pp. 124–134, 2019.

[8] M. Rasyid, B. H. Lee, and A. Sudarsono, "Wireless Body Area Network for Monitoring Body Temperature, Heart Beat and Oxygen in Blood," in *Proceedings of the International Seminar on Intelligent Technology & Its Applications*, Surabaya, Indonesia, May 2015.

[9] J. Yoon, Y. Jeong, H. Kim et al., "Robust and stretchable indium gallium zinc oxide-based electronic textiles formed by cilia-assisted transfer printing," *Nature Communications*, vol. 7, no. 1, Article ID 11477, 2016.

[10] J. Hao, A. Leblanc, L. Burgnies et al., "Textile split ring resonator antenna integrated by embroidery," *Electronics Letters*, vol. 55, no. 9, pp. 508–510, 2019.

[11] R. Quarfoth, Y. Zhou, and D. Sievenpiper, "Flexible patch antennas using patterned metal sheets on silicone," *IEEE Antennas and Wireless Propagation Letters*, vol. 14, pp. 1354–1357, 2015.

[12] J.-S. Roh, Y.-S. Chi, and T. J. Kang, "Wearable textile antennas," *International Journal of Fashion Design, Technology and Education*, vol. 3, pp. 135–153, 2010.

[13] R. Salvado, C. Loss, P. Pinho, and R. Gonçalves, "Textile materials for the design of wearable antennas A survey," *Sensors*, vol. 12, no. 11, Article ID 15841, 2012.

[14] W. Chaihongsa and C. Phongcharoenpanich, "Performance of textile antenna using two layers of strip line and round-off circular patch," in *Proceedings of the 2015 IEEE Conference on Antenna Measurements & Applications (CAMA)*, December 2015.

[15] A. Mersani and L. Osman, "Design of Dual-Band Textile Antenna for 2.45/5.8-GHz Wireless Applications," in *Proceedings of the 2016 5th International Conference on Multimedia Computing and Systems (ICMCS)*, Marrakech, Morocco, September 2016.

[16] A. Yadav, V. K. Singh, P. Yadav, A. K. Beliya, A. K. Bhoi, and P. Barsocchi, "Design of circularly polarized triple-band wearable textile antenna with safe low SAR for human health," *Electronics*, vol. 9, p. 1366, 2020.

[17] S. Sankaralingam and B. Gupta, "Development of textile antennas for body wearable applications and investigations on their performance under bent conditions," *Progress In Electromagnetics Research B*, vol. 22, no. 21, pp. 53–71, 2010.

[18] V. K. Singh and S. D. N. Bangari, "Wearable Ultra-wide Dual Band Flexible Textile Antenna for WiMax/WLAN Application," *Wireless Personal Communications*, vol. 95, 2017.

[19] M. A. R. Osman, M. K. Abd Rahim, M. Azfar Abdullah, N. A. Samsuri, F. Zubir, and K. Kamardin, "Design, implementation and performance of ultra-wideband textile antenna," *Progress In Electromagnetics Research B*, vol. 27, pp. 307–325, 2011.

[20] M. A. R. Osman, M. K. Abd Rahim, N. A. Samsuri, H. A. M. Salim, and M. F. Ali, "Embroidered fully textile wearable antenna for medical monitoring applications," *Progress in Electromagnetics Research*, vol. 117, pp. 321–337, 2011.

[21] P. B. Samal, P. J. Soh, and G. A. E. Vandenbosch, "UWB all-textile antenna with full ground plane for off-body WBAN communications," *IEEE Transactions on Antennas and Propagation*, vol. 62, no. 1, pp. 102–108, 2014.

[22] M. Kanagasabai, P. Sambandam, M. G. N. Alsath, S. Palaniswamy, A. Ravichandran, and C. Girinathan, "Miniaturized circularly polarized UWB antenna for body centric communication," *IEEE Transactions on Antennas and Propagation*, vol. 70, no. 1, pp. 189–196, 2022.

[23] P. H. Yu, "Effect of Sewing Types on Flexible Embroidery Antennas in UHF Band," in *Proceedings of the 2013 European Microwave Conference*, October 2013.

[24] R. A. Vatti, B. Arthi, P. Kumar, and R. Prabha, "Gain enhancement by utilizing hexagonal reflector based optimized textile antenna," *Journal of Ambient Intelligence and Humanized Computing*, 2021.

[25] S. Hasan, M. Sundaram, Y. Kang, and M. K. Howlader, "Measurement of Dielectric Properties of Materials Using Transmis sion/Reflection Method with Material Filled Transmission Line," in *Proceedings of the 2005 IEEE Instrumentation and Measurement Technology Conference*, pp. 22–27, Ottawa, ON, Canada, May 2005.

[26] S. H. Jing, D. Ding, and Q. X. Jiang, "Measurement of electromagnetic properties of materials using transmission/reflection method in coaxial line," in *Proceedings of the Asia-Pacific Conference on Environmental Electromagnetics*, pp. 590–595, Hangzhou, China, November 2003.

[27] Y. Li, W. Li, and Q. Ye, "A reconfigurable triple notch band antenna integrated with defected microstrip structure band-stop filter for ultra-wideband cognitive radio applications,"

International Journal of Antennas and Propagation, vol. 2013, Article ID 472645, 13 pages, 2013.

[28] Y. Li, W. Li, and W. Yu, "A switchable UWB slot antenna using SIS-HSIR and SIS-SIR for multi-mode wireless communications applications," *Applied Computational Electromagnetics Society Journal*, vol. 27, no. 4, pp. 340–351, 2012.

[29] Y. Li, W. Li, and Q. Ye, "A reconfigurable wide slot antenna integrated with SIRs for UWB/Multi-band communication applications," *Microwave and Optical Technology Letters*, vol. 55, no. 1, pp. 52–55, 2013.

[30] Y. Li, W. Li, and R. Mittra, "A compact CPW-fed circular slot antenna with reconfigurable dual band-notch characteristics for UWB communication applications," *Microwave and Optical Technology Letters*, vol. 56, no. 2, pp. 465–468, 2014.

[31] R. B. V. B. Simorangkir, A. Kiourti, and K. P. Esselle, "UWB wearable antenna with a full ground plane based on PDMS-embedded conductive fabric," *IEEE Antennas and Wireless Propagation Letters*, vol. 17, no. 3, pp. 493–496, 2018.

[32] M. Klemm, "Small patch antennas for UWB wireless body area network," *Ultra-Wideband, Short-Pulse Electromagnetics*, vol. 7, pp. 417–429, 2007.

[33] S. N. Mahmood, A. J. Ishak, T. Saeidi et al., "Full ground ultra-wideband wearable textile antenna for breast cancer and wireless body area network applications," *Micromachines*, vol. 12, no. 3, p. 322, 2021.

[34] M. Mustaqim, B. A. Khawaja, H. T. Chattha, K. Shafique, M. J. Zafar, and M. Jamil, "Ultra-wideband antenna for wearable Internet of Things devices and wireless body area network applications," *International Journal of Numerical Modelling: Electronic Networks, Devices and Fields*, vol. 32, no. 6, 2019.